INDIAN JOURNAL OF SCIENCE AND TECHNOLOGY

RESEARCH ARTICLE

Precursor Molarity Influence on Sprayed Mo-doped ZnO Films for solar cells

Sumalatha Chevva[1], Sreenivasulu Reddy Tirumalareddygari[2], Phaneendra Reddy Guddeti[1,3], Tulasi Ramakrishna Reddy Kotte[1]*

1 Solar Energy Laboratory, Department of Physics, Sri Venkateswara University, Tirupati-517502, India
2 Department of Physics, Viswam Engineering College, Madanapalle-517325, India
3 Department of Physics,, Dr. YSR Architecture and Fine Arts University, Kadapa-516002, India

OPEN ACCESS

Received: 30-04-2022
Accepted: 03-09-2022
Published: 21-09-2022

Citation: Chevva S, Tirumalareddygari SR, Guddeti PR, Reddy Kotte TR (2022) Precursor Molarity Influence on Sprayed Mo-doped ZnO Films for solar cells . Indian Journal of Science and Technology 15(36): 1800-1807. https://doi.org/10.17485/IJST/v15i36.842

* **Corresponding author**.

ktrkreddy@gmail.com

Funding: None

Competing Interests: None

Published By Indian Society for Education and Environment (iSee)

ISSN
Print: 0974-6846
Electronic: 0974-5645

Abstract

Objectives: Current research focuses on the role of precursor molarity effect on sprayed Mo-doped ZnO films and their suitability as window layers in solar cells. **Methods:** Molybdenum (Mo) doped zinc oxide (MZO) thin films were deposited by the technique of spray pyrolysis, varying the Zn molarity in the range, of 0.01 M to 0.20 M at a constant substrate temperature of 400 °C. The Mo doping concentration was constant at 2 at. %. **Findings:** The XPS studies witnessed the presence of Mo and Zn in +6 and +2 state respectively. The XRD pattern showed both (111) and (002) as strong peaks, confirming the hexagonal wurtzite crystal structure. The optical investigations showed that the MZO films with Zn molarity 0.10 M exhibited high optical transmittance having a wide energy band gap. Films with zinc molarity of 0.10 M showed low resistivity and high mobility. The prepared CTS/MZO hetero junction solar cells performance was studied by evaluating parameters such as open circuit voltage (V_{oc}) of 0.14 V, short circuit current density (J_{sc}) of 6.46 mA cm^{-2}, a fill factor (FF) of 0.27, and a conversion efficiency of 0.25 %. **Novelty:** Studies on the physical properties of Mo:ZnO layers such as Ritveld refinement analysis and Haze were reported first time. CTS/MZO hetero junction solar cells have not yet been published. The observed results are analogous to improve the efficiency of solar cells using environmentally benign materials.

Keywords: Spray pyrolysis; Thin films; XRD; Optical properties; Haze; Hall measurements

1 Introduction

Many investigations have been done for over from decades on transparent conducting oxide (TCO) thin layers for various applications in the field of science and technology [(1)]. The conventional TCOs found in the literature are InO_2 and SnO_2. They exhibit metallic forms of less content in the presence of hydrogen plasma [(2,3)], but ZnO films were found to be unchanging when exposed to hydrogen plasma [(4)]. ZnO films have gained a great deal attention due to its beneficial properties of less toxicity, small expansivity, wide

band gap (3.3 eV)[5] and its potential application as a TCO layer in light emitting diodes, flat panel displays, solar cells and chemical sensors[6–11].

In the literature there is an extensive study on MZO films using various transition metal ions such as Vanadium (V), Nickel (Ni), Niobium (Nb), Iron (Fe), Chromium (Cr), Gold (Au), Copper (Cu), Cobalt (Co), Zirconium (Zr), Molybdenum (Mo), Manganese (Mn), Titanium (Ti), and Halogens such as Chlorine (Cl) and Fluorine (F) and also some metalloids, metals such as Germanium (Ge), Boron (B), Bismuth (Bi), Aluminium (Al), Tin (Sn), Indium (In), and Gallium (Ga). However, the investigations reported on MZO thin films are meager, particularly in relation to deposition parameters. The valency difference between Mo^{6+} and Zn^{2+} ions is (+4), which will become very beneficial for doping ZnO with Mo. Each Molybdenum atom will provide four free electrons to the parent zinc lattice so that a small amount of Mo-doping can contribute more free electrons that could severely alter the electrical conductivity. Many thin film deposition techniques were used to grow MZO layers such as spray pyrolysis, and sputtering. To compare all these deposition techniques, spray pyrolysis is an easily adoptable technique for growing ZnO thin films over large areas and can be commercialized simple and low cost. Further, it is a method that no needs to create vacuum. In the present investigation zinc chloride was used as a precursor for zinc to deposit MZO layers instead of zinc acetate[12].

A detailed investigation of structural, morphological, optical, and electrical properties has been done in relation to Zn-precursor molarity. Rietveld refinement analysis and Haze analysis, which were previously unreported, were performed on Mo: ZnO layers. CTS/MZO heterojunction solar cells have not yet been reported. The observed results are comparable to improving the efficiency of solar cells through the use of environmentally friendly materials.

2 Methodology

MZO films were prepared using the spray pyrolysis technique on Corning 7059 glass substrates taking zinc chloride (Aldrich 98 %) as the zinc source and $MoCl_2$ (Aldrich 95 %) as the Mo source with methanol as solvent at a constant substrate temperature, 400 °C by changing Zn molarity in the range, 0.01 M – 0.20 M while the doping concentration of Mo was maintained constant 2 at. % (see Figure 1). The pH value of solution is varied 8.5±0.2 to 10±0.2 with Zn precursor molarity. The information regarding to the characterization techniques listed in our previous work[12].

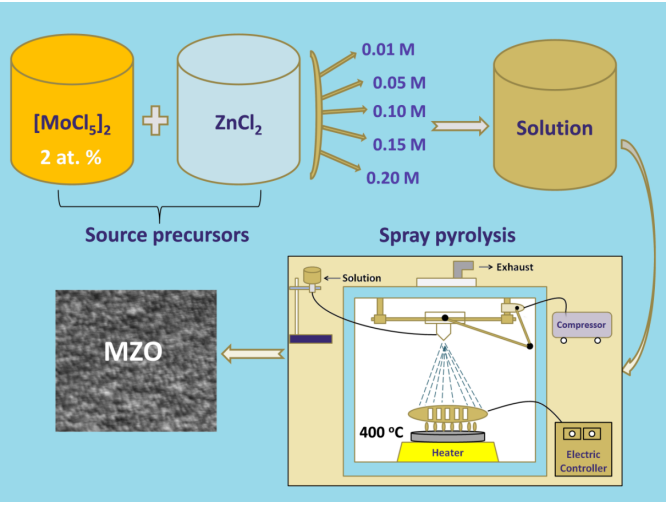

Fig 1. Experimental procedure used for deposition of MZO thin films via chemical spray pyrolysis technique.

3 Results and Discussions

3.1 XPS Analysis

For the evaluation of chemical composition of grown films and to know the valency state of Mo ion in ZnO lattice, X-ray photoelectron spectroscopy (XPS) spectra were recorded in the binding energy range 0-1350 eV. Figure 2 (a) shows MZO layers wide scan XPS spectrum grown with Zn molar concentration of 0.10 M at a substrate temperature of 400 °C. The peak observed at 307.43 eV is corresponding to C 1s. The spectrum exhibited two strong peaks at 1021.24 eV and 1044.42 eV, which

corresponding to the binding energies of $Zn2p_{3/2}$ and $Zn2p_{1/2}$ respectively. The peak observed at 530.26 eV is related to lattice oxygen and represents O1s combined with Mo and Zn atoms. Due to the increase of Zn^{2+} and Mo^{6+} ions during the film deposition, a sufficient number of oxygen atoms in the atmosphere can diffuse into the ZnO lattice and occupy oxygen vacancies.

3.2 XRD Analysis

The XRD patterns of grown MZO layers using different precursor molar concentrations with Mo-doping of 2 at. % was shown in Figure 2 (b). The XRD pattern depicts the polycrystalline nature of the films. XRD patterns of the films prepared at different Zn- concentrations, varying from to 0.01 M to 0.20 M show peaks at 30.98°, 31.12°, 34.33°, 36.07°, 47.04°, 62.57°, 67.39° corresponding to (111), (100), (002), (021), (102), (103), and (112) planes. Among these planes, (100), (002), (102), (103), and (112) planes were related to the ZnO hexagonal wurtzite structure and these results were closely matched with the JCPDS card No. 74-0534. Further, the (111) and (021) planes present in the spectra corresponded to monoclinic structure of MZO and agrees well with the JCPDS card No. 25-1024.

The analysis of Rietveld refinement was also done to know the presence of Mo in ZnO lattice, for MZO films prepared using a Zn- molar concentration of 0.15 M. In addition, R weighted profile (R_{wp}), R profile (R_p), R structure factor, R Bragg factor (R_{Bragg}), goodness of fit (GOF) such structural parameters were also calculated. EXPO software was used to calculate the unit cell parameters from the Rietveld refinement data.

The calculated Rietveld refinement parameters such as R_p, R_{wp}, GOF, R structure factor, R_{Bragg}, and unit cell parameters were listed in Table 1. As the GOF value is 1.57 one can clearly speak about the quality of the data used to refine. Table 2 shows the site occupancies of ions distributed along fractional coordinates. The extracted crystal structure of MZO is shown in Figure 2 (c) (inset). MZO contains one Mosite (Mo1), one Zn site (Zn1) and two O sites (O1 and O2). The unit cell lattice parameters were also listed in Table 1.

Calculated lattice structure and refinement parameters from Rietveld refinement pattern for MZO film prepared at 0.15 M of Zn- concentration.

Table 1. Calculated lattice structure and refinement parameters from Rietveld refinement patternfor MZO film prepared at 0.15 Mof Zn-concentration.

Unit cell parameters	
a, (Å)	4.69
b, (Å)	5.73
c, (Å)	4.89
α ,(°)	90
β, (°)	90.31
γ, (°)	90
Cell volume $(Å)^3$	131.27
Volume per atom $(Å)^3$	10.94
Density (g/cm^3)	5.70
Crystal system & Space group number	Monoclinic & (P1c1)
Laue group & Point group symbols	2/m &2/ m
Structure parameters	
Atoms	28
Bonds	24
Polyhedra	06
Refinement parameters	
R_p	7.651
R_{wp}	12.065
Goodness of fit	1.57
R-Structure factor	47.884
R-Bragg factor	64.834

The lattice parameters were evaluated by following expressions (1) to (3) mentioned below[13]

Table 2. The site occupancies of various ions along with their fractional coordinates

Element	X	Y	Z	Occupancy
Mo1	0.0000	0.8119	0.2500	1.000
Zn1	0.5000	0.6918	0.7500	1.000
O1	0.2538	0.6236	0.4014	1.000
O2	-0.2165	0.8950	0.5603	1.000

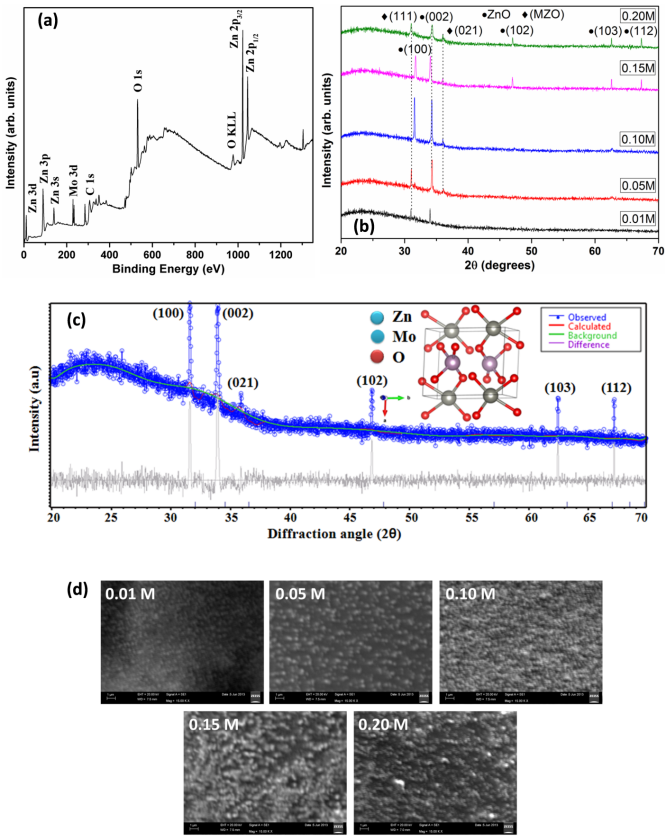

Fig 2. (a) XPS Typical wide scan and core level spectrum of MZO films grown at 400 °C with a Zn molarity of 0.10 M. (b) XRD pattern of MZO films formed at a substrate temperature of 400 °C using different Zn- molar concentrations. (c) Rietveld refinement pattern of the Monoclinic MZO film prepared at 0.15 M of Zn- concentration. (d) SEM pictures of MZO films prepared using different Zn molarities.

The lattice parameters were measured and it can be seen that the value of the lattice constant and the interplanar distance (d) are decreased by increasing the molar concentration of the precursor present in the growth film.

From the data obtained, it is found that MZO films with a starting solution molarity of 0.10 M showed minor change in the lattice parameters with a = 0.326 nm, c = 0.563 nm and d = 0.282 nm. The Debye-Scherrer formula[13] was used to calculate crystallite size (D) of the grown films.

where β represents full width at half maximum (FWHM) in radians, θ represents angle of diffraction, λ represents X-rays wavelength and 'n' represents the correction factor (n = 0.9), The evaluated values are tabulated (see Table 3). The value of D increased up to 0.10 M and then decreased with increase of Zn molarity. Which clearly depicts the increase of Zn molarity could disgrace the crystallinity of the films. Similar results were reported by Masumdar et. al for sprayed ZnO thin films[14]. Then the dislocation density (δ) in the grown films was evaluated from the following relation

The evaluated (δ) values are tabulated in Table 3. The dislocation density value decreased up to 0.10 M precursor molarity and increased thereafter, it is clear that the films grown at 0.10 M were of good quality with less number of defects present. The change in lattice strain (ε) causes lattice mismatch between the substrate and thin film, which can be evaluated using the

following expression,

where θ represents angle of diffraction and β represents full width at half maximum (FWHM) in radians. The films with precursor molar concentration 0.10 M exhibited low value of ε, indicates less defects between the grown MZO films and substrate. Further the lattice strain increases for higher precursor molar concentrations. This might be due to variation of nucleation mechanism in the films. Polycrystalline films preferential orientation can be obtained by evaluating texture coeffcient T_c, which is evaluated using the below expression (7)

where $I_{(hkl)}$ is the relative intensity measured on the preferred orientation plane (hkl) and N is the number of reflections observed on the XRD graph. $I_{0(hkl)}$ represents standard diffraction pattern (JCPDS: 750576) intensity. It is found from the values obtained that MZO films grown with 0.10 M of precursor solution exhibited a high T_c and less lattice defects than other MZO films, which shows that for precursor solution of 0.10 M more number of crystallites of MZO layers are oriented along the (002) plane. The Lorentz factor greatly influences peak intensity, which depends on the integrated intensity. Lorentz factor can be evaluated using the following formula.

where θ represents the angle of diffraction. The evaluated values of L are tabulated (see Table 3). The disordering of crystallographic planes will be characterized by planar defects. These are taken as stacking faults. Stacking faults of deposited films were determined by using the relation given below

where θ represents the angle of diffraction and β represents the FWHM. The evaluated Stacking faults values are tabulated (see Table 3). The layers deposited at a Zn molarity of 0.10 M in the starting solution exhibited low SF value compared with other thin films. In high band gap materials, the crystal band structure forms an energy barrier and impedes electron transport of semiconductor components.

Table 3. Structural parameters of MZO films grown with different precursor molarities.

Precursor molarity (M)	Crystal plane (hkl)	Crystallite size, D (nm)	Dislocation density ($\times 10^{15}$)	Lattice strain, ε	Texture coefficient (T_c)	Lorentz factor	Stacking fault (SF)
0.01	(002)	9.26	11.66	0.0036	5.31	3.02	0.0092
0.05	(002)	55.20	0.32	0.0008	5.67	3.25	0.0024
0.10	(002)	84.47	0.14	0.0004	6.51	3.55	0.0008
0.15	(002)	52.35	0.36	0.0007	2.96	2.80	0.0019
0.20	(002)	8.46	13.97	0.0040	2.60	2.07	0.0076

3.3 Morphological properties

Figure 2 (d) represents the SEM images of different molar Zn concentrations of the grown MZO layer and the distribution of the particles on glass surface. All films displayed ”nut-shaped” particles growing on the surface of the substrate. The size of the grain obtained is strongly influenced by the change in the molar concentration of Zn. Because of this, the grain size in the deposited films increased from 70 nm to 450 nm with Zn molarity, the average grain size is 240 nm. The films prepared at Zn molarity of 0.10 M shows the densely packed grains without any voids, this can help improve the solar cell's performance.

3.4 Optical properties

Figure 3 (a) shows the transmittance (t %) of the films grown at different starting zinc solution molarity. The deposited layers were showed good transmittance in the visible region. An average transmittance of 80% was observed in all the grown films. It is very clear that at higher zinc molar concentration, the films showed low optical transmittance. The decrement of t % at higher molar concentration is due to rough surface and the film color changes from whitish to gray. Obviously the rough surface causes light scattering to occur with a reduction in transmittance. The better transmittance observed for the film grown with Zn molar concentration of 0.10 M is due to the more active mass deposited on the substrate at this particular solution concentration. The absorption coefficient (α) of deposited films was calculated from the expression given below.(10)

Here, t represents the thickness of the film. The thickness of the film was taken as 500 nm. The energy band gap (E_g) of the grown layers was evaluated by the following expression,

where A is a constant, $h\upsilon$ represents the energy of photon and n=1/2 shows a direct optical transition in these deposited films.

Figure 3 (b) shows the plots of $(\alpha h\upsilon)^2$ versus $h\upsilon$. The $(\alpha h\upsilon)^2$ plots are is a linear function of energy ($h\upsilon$) for all the films. Extrapolation of linear portion of this plot on to the energy axis gives the energy band gap. It can be observed that all the

films exhibited direct allowed transition and the band gap varied from 2.7 eV to 3.65 eV with the zinc precursor concentration increasing from 0.01 M to 0.20 M. The evaluated energy band gap values are in good agreement with the results reported by others in the literature.

3.5 Haze

The ratio of intensity of diffused light to the total intensity of transmitted and reflected light on textured interface is called Haze. It predicts the degree of scattering of light. The Haze value can be calculated from following relation,(12)

The change of Haze parameter with wavelength in air medium is shown in Figure 3(c).

The scattering phenomena always influenced by the incident medium refractive index, magnitude of light and interface morphology.[15]. Figure 3(c) shows, the values of Haze vary in the range, 0.18 – 0.89 for grown MZO layers of different Zn molarities. From Figure 3 (c), it is clear that for a Zn molarity of 0.10 M, the MZO films showed less haze compared with films formed at other Zn concentrations. One can observe the increase of Haze value with Zn molarity in the MZO films, which confirms the dependence of surface roughness with Zn molarity. Films made with a Zn molar concentration of 0.10 M showed little haze and less light scattering due to the presence of nutty particles over the entire film surface of these layers.

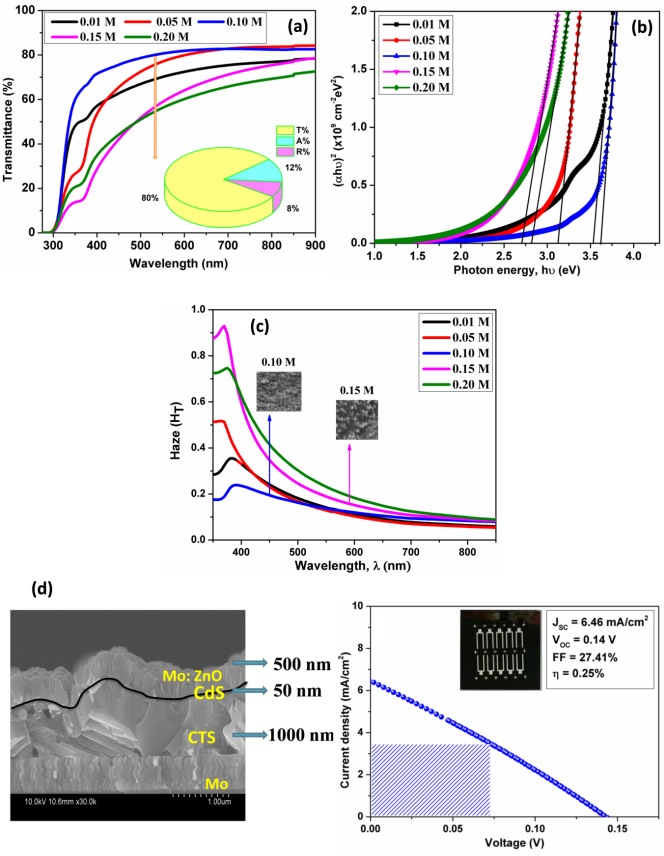

Fig 3. (a) Optical transmission versus wavelength spectra of MZO films prepared using different starting solution molar concentrations. (b) $(\alpha h\upsilon)^2$ versus $(h\upsilon)$ plots for MZO films. (c) Haze parameter (measured in air) of ZnO:Mo films prepared using different Zn molarity concentrations. The related SEM picture of film surface is shown in the inset. (d) Cross-section images of the MZO device prepared at 0.10 M. and J-V characteristics of solar cells.

3.6 Electrical properties

The Hall measurements clearly showed n-type conductivity for all MZO films with resistivity varying from 15×10^{-2} Ωcm to 1.9×10^{-2} Ωcm with carrier concentration varying in the range, 2.28- 7.8×10^{18} cm^{-3} and carrier mobility changing between

15cm^2/V-s and 42 cm^2/V-s (See Table 4). The electrical resistivity of the films decreased with increase of solution molarity and stabilized at a value of 0.10 M. Further, at higher precursor molarity, the resistivity increased due to poor crystallinity. The carrier density of the grown films increased and reached a maximum at 0.10 M. The carrier mobility of the deposited films increased and reached a maximum for the solution molarity of 0.10 M. The similar results were reported by Gokulakrishnan et al.[16].

Table 4. Dependence of the electrical resistivity (ρ), carrier concentration (N), and mobility (μ) of MZO films at different Zn molar concentrations.

Zn molar concentration (M)	Resistivity (Ω-cm)	Carrier density (cm^{-3})	Hall mobility(cm^{2}V^{-1}s^{-1})
0.01	15.3 x10^{-2}	3.88 x10^{18}	15
0.05	5.4 x10^{-2}	5.7 x10^{18}	20.32
0.10	1.9 x10^{-2}	7.8x10^{18}	42
0.15	4.1 x10^{-2}	4.4 x10^{18}	34.46
0.20	9.3 x10^{-2}	2.28 x10^{18}	29.52

3.7 J-V characteristics of solar cells

In order to test the potentiality of the optimized MZO window layer, a hetero-junction solar cell was fabricated in substrate configuration with the device structure, SLG/Mo/Cu_2SnS_3/CdS/Mo:ZnO/Au/Cu. The schematic diagram of the junction cross-section is shown in Figure 3 (d). In the device fabrication, Mo back contact layers were grown using DC magnetron sputtering. The CTS absorber layers of 1000 nm thickness were deposited using two-stage process. Chemical bath deposited CdS (50 nm) was used as the buffer layer. The MZO layer layer of 500 nm was used as window layer. Finally, the Au/Cu bilayer top contacts were grown using thermal evaporation technique. The current density-voltage (J - V) characteristics of prepared solar cells under illumination with a light source of 100 mWcm^{-2} at AM 1.5 conditions are shown in Figure 3 (d).

The fabricated solar cells exhibited an open circuit voltage (V_{oc}) of 0.14 V, short circuit current density (J_{sc}) of 6.46 mA cm^{-2}, a fill factor (FF) of 0.27, and a conversion efficiency of 0.25 %. In general, the quality of the absorber decides performance of the device. The collection of more number of charge carriers is mainly depends on the uniform and homogeneous surface of the absorber layer in which no voids[17], also decrease of recombination losses in the short circuit current[18,19]. Furthermore, the main problem is the deep absorber defects, which reduce the saturation current density (Jo) and the open circuit voltage, leading to a reduced duty cycle. Therefore, the poor quality of severely defective absorbers can be the reason for the poor performance of the device in this task. However, this is an initial attempt to make a device using MZO layers grown in this work. However, the observed low conversion efficiency can be improved in future by optimizing various absorber and buffer layer parameters.

4 Conclusion

MZO layers were successfully deposited by chemical spray pyrolysis technique by varying the zinc precursor molar concentration in the range, 0.01 – 0.20 M maintaining a constant substrate temperature of 400 °C and dopant Mo content of 2 at. % constant. The comprehensive structural, optical and electrical properties of the films prepared at different Zn precursor concentrations were studied. The as deposited MZO films were polycrystalline in nature and exhibiting hexagonal wurtzite structure with (002) preferred orientation. The energy band gap values of the films varied in the range, 2.70 to 3.65 eV, respectively with the change of Zn- molar concentration. Investigation of electrical properties showed that the films grown at 0.10 M precursor concentration exhibited a low resistivity of 1.9x10^{-2} Ωcm, high mobility 42 cm^2/V-S and carrier concentration 7.8x10^{18} cm^{-3} Compared to other films. Hence, MZO films grown at 0.10 M precursor concentration with a Mo content of 2 at. % exhibited better opto-electrical properties that could be used as window layers in hetero-junction photovoltaic cells. Hetero-junction solar cell was fabricated with MZO film as a window layer that showed photovoltaic response.

5 Authors contribution

Sumalatha Chevva, Sreenivasulu Reddy Tirumalareddygari and Phaneendra Reddy Guddeti have equally contributed to this work

References

1) Buryi M, Remeš Z, Babin V, Chertopalov S, Děcká K, Dominec F, et al. Free-Standing ZnO:Mo Nanorods Exposed to Hydrogen or Oxygen Plasma: Influence on the Intrinsic and Extrinsic Defect States. *Materials*. 2022;15(6):2261–2261. Available from: https://doi.org/10.3390/ma15062261.
2) Fang Y, Commandeur D, Lee WC, Chen Q. Transparent conductive oxides in photoanodes for solar water oxidation. *Nanoscale Advances*;2(2):626–632. Available from: https://doi.org/10.1039/C9NA00700H.
3) Goyal D, Solanki P, Marathe B, Takwale M, Bhide V. Deposition of Aluminum-Doped Zinc Oxide Thin Films by Spray Pyrolysis. *Japanese Journal of Applied Physics*. 1992;31(Part 1, No. 2A):361–364. Available from: https://doi.org/10.1143/JJAP.31.361.
4) Major S, Kumar S, Bhatnagar M, Chopra KL. Effect of hydrogen plasma treatment on transparent conducting oxides. *Applied Physics Letters*. 1986;49(7):394–396. Available from: https://doi.org/10.1063/1.97598.
5) Goyal D, Takwale MG, Bhide VG. National solar energy Convention. New Delhi. Tata McGraw-Hill. 1990;p. 218–218.
6) Owoeye EVA, Ajenifuja A, Adeoye AOE, Salau S, Adewinbi A. Effect of precursor concentration on corrosion resistance and microstructure of ZnO thin films using spray pyrolysis method. *Scientific African*. 2022;p. e01073. Available from: https://doi.org/10.1016/j.sciaf.2021.e01073.
7) Alam MW, Ansari MZ, Aamir M, Waheed-Ur-Rehman M, Parveen N, Ansari SA. Preparation and Characterization of Cu and Al Doped ZnO Thin Films for Solar Cell Applications. *Crystals*;12(2):128–128. Available from: https://doi.org/10.3390/cryst12020128.
8) Mansouri F, Khaaissa Y, Abdelalitalbi K, Nouneh. Molarity Dependent on CVD Misted ZnS Buffer Layer Performance. *International Journal of Thin Film Science and Technology*. 2021;10(3):239–248. Available from: http://dx.doi.org/10.18576/ijtfst/100314.
9) Hat AE, Chaki I, Essajai R, Mzerd A, Schmerber G, Regragui M, et al. Growth and Characterization of (Tb,Yb) Co-Doping Sprayed ZnO Thin Films. *Crystals*. 2020;10(3):169–169. Available from: https://doi.org/10.3390/cryst10030169.
10) Speaks DT. Effect of concentration, aging, and annealing on sol gel ZnO and Al-doped ZnO thin films. *International Journal of Mechanical and Materials Engineering*. 2020;15(1). Available from: https://doi.org/10.1186/s40712-019-0113-6.
11) Shishiyanu ST, Shishiyanu TS, Lupan OI. Sensing characteristics of tin-doped ZnO thin films as NO2 gas sensor. *Sensors and Actuators B: Chemical*. 2005;107(1):379–386. Available from: https://doi.org/10.1016/j.snb.2004.10.030.
12) Hichou AE, Addou M, Ebothé J, Troyon M. Influence of deposition temperature (Ts), air flow rate (f) and precursors on cathodoluminescence properties of ZnO thin films prepared by spray pyrolysis. *Journal of Luminescence*. 2005;113(3-4):183–190. Available from: https://doi.org/10.1016/j.jlumin.2004.09.123.
13) Ozgur U, Alivov YI, Liu C, Teke A, Reshchikov MA, Dogan S, et al. A comprehensive review of ZnO materials and devices. *JAppl Phys*. 2005. Available from: https://doi.org/10.1063/1.1992666.
14) Joseph BG, Gopchandran KG, Manoj PK, Koshy PK, Vaidyan VK. Optical and electrical properties of zinc oxide films prepared by spray pyrolysis. *Bulletin of Materials Science*. 1999;22(5):921–926. Available from: https://doi.org/10.1007/BF02745554.
15) Krc J, Lipovsek B, Bokalic M, Campa A, Oyama T, Kambe M, et al. Potential of thin-film silicon solar cells by using high haze TCO superstrates. *Thin Solid Films*. 2010;518(11):3054–3058. Available from: https://doi.org/10.1016/j.tsf.2009.09.164.
16) Gokulakrishnan V, Parthiban S, Jeganathan K, Ramamurthi K. Investigation of Molybdenum Doped ZnO Thin Films Prepared by Spray Pyrolysis Technique. *Ferroelectrics*. 2011;423(1):126–134. Available from: https://doi.org/10.1080/00150193.2011.620898.
17) He M, Lokhande AC, Kim IY, Ghorpade UV, Suryawanshi MP, Kim JH. Fabrication of sputtered deposited Cu2SnS3 (CTS) thin film solar cell with power conversion efficiency of 2.39 %. *Journal of Alloys and Compounds*. 2017;701:901–908. Available from: https://doi.org/10.1016/j.jallcom.2017.01.191.
18) Chaudhari JJ, Joshi US. Fabrication of high quality Cu₂SnS₃thin film solar cell with 1.12% power conversion efficiency obtain by low cost environment friendly sol-gel technique. *Materials Research Express*. 2018;5(3):036203–036203. Available from: https://doi.org/10.1088/2053-1591/aab20e.
19) Dahman H, Mir LE. Cu2SnS3 thin films deposited by spin coating route: a promise candidate for low cost, safe and flexible solar cells. *Journal of Materials Science: Materials in Electronics*. 2015;26(8):6032–6039. Available from: https://doi.org/10.1007/s10854-015-3180-3.